Optimizing photonic crystal waveguides for on-chip spectroscopic applications

Andreas C. Liapis,[1,*] **Zhimin Shi,**[1,2] **and Robert W. Boyd**[1,3,4]

[1]*The Institute of Optics, University of Rochester, Rochester, NY 14627, USA*
[2]*Department of Physics, University of South Florida, Tampa, FL 33620, USA*
[3]*Department of Physics and Astronomy, University of Rochester, Rochester, NY 14627, USA*
[4]*Department of Physics and School of Electrical Engineering and Computer Science, University of Ottawa, Ottawa, ON K1N 6N5, Canada*

[*]*liapis@optics.rochester.edu*

Abstract: We investigate the applicability of photonic crystal waveguides to high-resolution on-chip spectrometers. We argue that the figure of merit by which their performance should be gauged is not the group index bandwidth product, which photonic crystal waveguides are usually optimized for, but the working finesse, which relates to the maximum number of spectral lines resolvable by a slow-light spectrometer. Through numerical simulation, we show that a properly-optimized photonic crystal waveguide could form the basis of a spectrometer with a spectral resolution of 0.04 nm over a 12.5 nm bandwidth near 1550 nm and with a footprint six times smaller than a conventional spectrometer.

OCIS codes: (130.5296) Photonic crystal waveguides; (300.6190) Spectrometers.

References and links

1. M. K. Smit and C. Van Dam, "PHASAR-Based WDM-Devices: Principles, Design and Applications," IEEE J. Quantum Electron. **2**(2), 236–250 (1996).
2. B. Momeni, E. S. Hosseini, M. Askari, M. Soltani, and A. Adibi, "Integrated photonic crystal spectrometers for sensing applications," Opt. Commun. **282**(15), 3168–3171 (2009).
3. Z. J. Sun and K. A. McGreer, "Demultiplexer with 120 channels and 0.29-nm channel spacing," IEEE Photon. Technol. Lett. **10**(1), 90–92 (1998).
4. B. B. C. Kyotoku, L. Chen, and M. Lipson, "Sub-nm resolution cavity enhanced microspectrometer," Opt. Express **18**(1), 102–107 (2010).
5. C. Z. Zhao, G. Z. Li, E. K. Liu, Y. Gao, and X. D. Liu, "Silicon on insulator Mach-Zehnder waveguide interferometers operating at 1.3 m," Appl. Phys. Lett. **67**(17), 2448–2449 (1995).
6. S.-W. Wang, C. Xia, X. Chen, W. Lu, M. Li, H. Wang, W. Zheng, and T. Zhang, "Concept of a high-resolution miniature spectrometer using an integrated filter array," Opt. Lett. **32**(6), 632–634 (2007).
7. Z. Xia, A. A. Eftekhar, M. Soltani, B. Momeni, Q. Li, M. Chamanzar, S. Yegnanarayanan, and A. Adibi, "High resolution on-chip spectroscopy based on miniaturized microdonut resonators," Opt. Express **19**(13), 12356–12364 (2011).
8. X. Gan, N. Pervez, I. Kymissis, F. Hatami, and D. Englund, "A high-resolution spectrometer based on a compact planar two dimensional photonic crystal cavity array," Appl. Phys. Lett. **100**(23), 231104 (2012).
9. P. B. Deotare, L. Kogos, Q. Quan, R. Ilic, and M. Loncar, "On-chip integrated spectrometer using nanobeam photonic crystal cavities," in *CLEO: Science and Innovations*, OSA Technical Digest (online) (Optical Society of America, 2012), paper CM3B.4.
10. W. Jiang, K. Okamoto, F. M. Soares, F. Olsson, S. Lourdudoss, and S. J. B. Yoo, "5 GHz Channel Spacing InP-Based 32-Channel Arrayed-Waveguide Grating," in *Optical Fiber Communication Conference*, OSA Technical Digest (CD) (Optical Society of America, 2009), paper OWO2.
11. Z. Shi and R. W. Boyd, "Slow-light enhanced spectrometers on chip," Proc. SPIE **8007,** 80071D (2011).
12. Z. Shi, R. W. Boyd, D. J. Gauthier, and C. C. Dudley, "Enhancing the spectral sensitivity of interferometers using slow-light media," Opt. Lett. **32**(8), 915–917 (2007).

#184499 - $15.00 USD Received 4 Feb 2013; revised 6 Apr 2013; accepted 8 Apr 2013; published 16 Apr 2013

13. Z. Shi, R. W. Boyd, R. M. Camacho, P. K. Vudyasetu, and J. C. Howell, Slow-light Fourier transform interferometer, Phys. Rev. Lett. **99**(24), 240801 (2007).
14. Z. Shi and R. W. Boyd, "Slow-light interferometry: practical limitations to spectroscopic performance," J. Opt. Soc. Am. B **25**(12), C136–C143 (2008).
15. R. Jacobsen, A. Lavrinenko, L. Frandsen, C. Peucheret, B. Zsigri, G. Moulin, J. Fage-Pedersen, and P. Borel, "Direct experimental and numerical determination of extremely high group indices in photonic crystal waveguides," Opt. Express **13**(20), 7861–7871 (2005).
16. L. H. Frandsen, A. V. Lavrinenko, J. Fage-Pedersen, and P. I. Borel, "Photonic crystal waveguides with semi-slow light and tailored dispersion properties," Opt. Express **14**(20), 9444–9450 (2006).
17. Y. Hamachi, S. Kubo, and T. Baba, "Slow light with low dispersion and nonlinear enhancement in a lattice-shifted photonic crystal waveguide," Opt. Lett. **34**(7), 1072–1074 (2009).
18. J. Sancho, J. Bourderionnet, J. Lloret, S. Combrié, I. Gasulla, S. Xavier, S. Sales, P. Colman, G. Lehoucq, D. Dolfi, J. Capmany, and A. De Rossi, "Integrable microwave filter based on a photonic crystal delay line," Nat. Commun. **3,** 1075 (2012).
19. S. A. Schulz, L. O'Faolain, D. M. Beggs, T. P. White, A. Melloni, and T. F. Krauss, "Dispersion engineered slow light in photonic crystals: a comparison," J. Opt. **12**(10), 104004 (2010).
20. H. Lotfi, N. Granpayeh, and S. A. Schulz, "Photonic crystal waveguides with ultra-low group velocity," Opt. Commun. **285**(10), 2743–2745 (2012).
21. F. Wang, J. S. Jensen, and O. Sigmund, "High-performance slow light photonic crystal waveguides with topology optimized or circular-hole based material layouts," Photon. Nanostruct.: Fundam. Appl. **10**(4), 378–388 (2012).
22. Z. Shi and R. W. Boyd, "Fundamental limits to slow-light arrayed-waveguide-grating spectrometers," Opt. Express **21**(6), 7793 (2013).
23. E. Kuramochi, M. Notomi, S. Hughes, A. Shinya, T. Watanabe, and L. Ramunno, "Disorder-induced scattering loss of line-defect waveguides in photonic crystal slabs," Phys. Rev. B **72**(16), 161318 (2005).
24. S. Hughes, L. Ramunno, J. F. Young, and J. E. Sipe, "Extrinsic Optical Scattering Loss in Photonic Crystal Waveguides: Role of Fabrication Disorder and Photon Group Velocity," Phys. Rev. Lett. **94**(3), 033903 (2005).
25. L. O'Faolain, S. A. Schulz, D. M. Beggs, T. P. White, M. Spasenović, L. Kuipers, F. Morichetti, A. Melloni, S. Mazoyer, J. P. Hugonin, P. Lalanne, and T. F. Krauss, "Loss engineered slow light waveguides," Opt. Express **18**(26), 27627–27638 (2010).
26. Available online at: *www.st-andrews.ac.uk/microphotonics*
27. S. G. Johnson and J. D. Joannopoulos, "Block-iterative frequency-domain methods for Maxwell's equations in a planewave basis," Opt. Express **8**(3), 173–190 (2001).
28. M. Patterson, S. Hughes, S. Schulz, D. M. Beggs, T. P. White, L. OFaolain, and T. F. Krauss, "Disorder-induced incoherent scattering losses in photonic crystal waveguides: Bloch mode reshaping, multiple scattering, and breakdown of the Beer-Lambert law," Phys. Rev. B **80**(19), 195305 (2009).
29. J. Topolancik, B. Ilic, and Frank Vollmer, "Experimental observation of strong photon localization in disordered photonic crystal waveguides," Phys. Rev. Lett. **99**(25), 253901(2007).
30. M. Patterson, S. Hughes, S. Combrié, N-V-Q. Tran, A. De Rossi, R. Gabet, and Y. Jaouën, "Disorder-induced coherent scattering in slow-light photonic crystal waveguides," Phys. Rev. Lett. **102**(25), 253903 (2009).

1. Introduction

In recent years, the demand for molecular and biological detection and identification has increased, making the development of miniaturized spectrometers a worthwhile pursuit. Considerable effort has been put towards answering this demand and, amongst the various implementations reported, two broad types of spectrometers are discerned:

Firstly, there are integrated interferometric spectrometers, such as arrayed-waveguide grating (AWG) spectrometers [1], superprism spectrometers [2], grating-based spectrometers [3, 4], and on-chip implementations of the Mach-Zehnder geometry [5]. As these rely on dispersive elements for their operation, their spectral resolution is limited by the size of the dispersive region.

Secondly, there are arrays of cascaded optical elements with narrow-band spectral responses, such as Fabry-Perot filters [6], microdonut resonators [7], photonic crystal cavities [8, 9], etc. In spectrometers of this second type, the spectral resolution is limited by the width of the frequency response of the individual elements, while their free spectral range limits the total number of resolvable spectral lines. For example, Xia *et al.*, have reported a spectral resolution of ~ 0.5 nm over a ~ 50 nm bandwidth in a spectrometer with a footprint of ~ 1 mm^2 [7].

#184499 - $15.00 USD Received 4 Feb 2013; revised 6 Apr 2013; accepted 8 Apr 2013; published 16 Apr 2013

In comparison, the current state of the art in interferometric spectrometers gives a spectral resolution of ~ 0.04 nm over a 1.3 nm bandwidth but with a device size of the order of square centimeters [10]. Reducing the footprint of interferometric spectrometers is vital, if such spectrometers are to be integrated in future lab-on-a-chip devices [11].

It has recently been shown that slow-light methods can be used to enhance the spectral resolution of various types of spectrometers by a factor as large as the group index [12–14]. The application of such methods to integrated photonic devices could allow us to further reduce the footprint of on-chip spectrometers without sacrificing their performance. In this paper we investigate the applicability of photonic crystal waveguides to spectroscopic applications by taking into account both their group index and the associated loss.

2. On-chip slow light

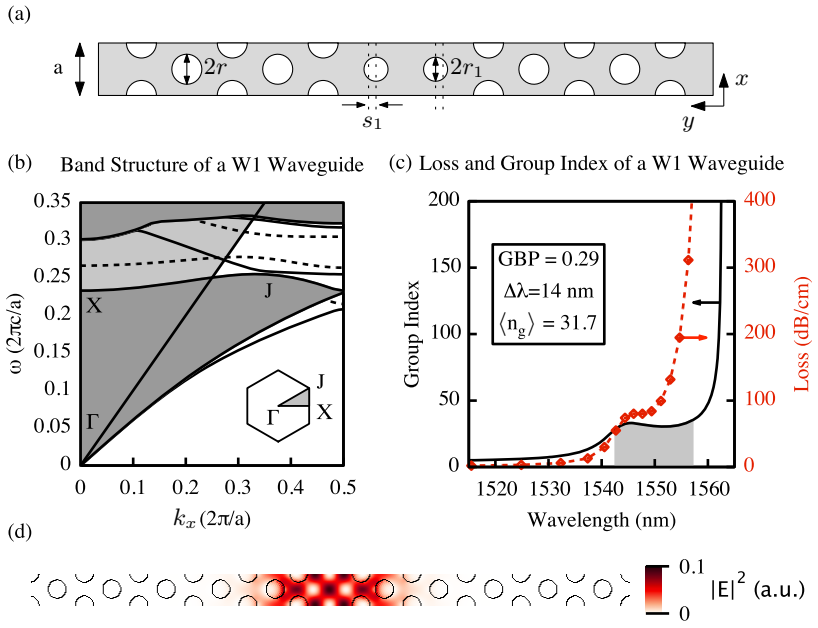

Fig. 1. Schematic (a), dispersion diagram (b) and group-index profile and calculated propagation loss (c) of a W1 Silicon photonic crystal waveguide designed to have a constant group index $\langle n_g \rangle = 31.7$ over a 14 nm bandwidth. Areas of the dispersion diagram shaded dark grey indicate modes of the bulk photonic crystal, whose first Brillouin Zone is shown in the inset. Modes above the light line (light grey shading) will leak energy out of the slab. Guided modes are labeled even (solid) or odd (dashed) based on their symmetry properties. The operating bandwidth of this device is indicated by the shaded area in (c). The distribution of $|E|^2$ in the slow-light regime is shown in (d).

Photonic crystal line-defect waveguides (PhCWs) are one of the most prominent on-chip slow-light methods. W1 waveguides, in particular, which are formed by removing one row of holes from a triangular-lattice photonic crystal, have been shown to have group indices near the band edge of the order of 200, albeit with significant group-velocity dispersion (GVD) [15]. For delay-line applications it is desirable to minimize the GVD over the operating frequency range of the device, such that signals are not significantly distorted after passing through the device.

#184499 - $15.00 USD Received 4 Feb 2013; revised 6 Apr 2013; accepted 8 Apr 2013; published 16 Apr 2013

To that end, the waveguide's dispersion profile is tailored by suitably shifting and scaling the holes adjacent to the line defect (Fig. 1) [16–18]. By properly optimizing the geometry, it is possible to engineer a plateau in the group-index profile [see, e.g. Fig. 1(c)], the bandwidth of which can be increased at the expense of the group-index value.

In designing such waveguides, the most commonly used figure of merit is the group index bandwidth product (GBP) [19], $\langle n_g \rangle \Delta\omega/\omega_0$, where the bandwidth $\Delta\omega$ is defined as the frequency range centered at ω_0 over which the group index remains within 10% of its average value $\langle n_g \rangle$. This can be thought of as a length-independent equivalent to the delay-bandwidth product, and can be used to evaluate the waveguide's performance in slow-light delay-line applications. Considerable effort has been put towards optimizing the design of PhCWs for this figure of merit, with typical values in the range of 0.1 - 0.4 for an optimized W1 geometry [19] and up to 0.5 for more exotic designs [20, 21]. The group index bandwidth product is not, however, the most pertinent figure of merit for spectroscopic applications, as it does not take into account propagation losses.

3. The characteristic spectral resolution and working finesse of PhCWs

In the ideal case of lossless propagation, the spectral resolution of a slow-light spectrometer, which is proportional to the size of the structure, is unbounded, as the characteristic length of the slow-light medium can be made arbitrarily large. For any realistic device, however, the effects of loss must be considered. The performance of slow-light spectrometers in the presence of loss has been studied for various spectrometer configurations, and is found to be bounded by the ratio of the group index n_g of the slow-light medium to the associated loss α [14, 22]. This quantity, $c\alpha/n_g$, which we hereafter refer to as the characteristic spectral resolution $\delta\omega$, allows us to assess the performance of the slow-light medium independently of the specific geometry of the spectrometer in which it is used.

The dispersion of this quantity limits the useful working bandwidth. We therefore propose optimizing the geometry of PhCWs for the working finesse $\mathscr{F}_W$, defined as the ratio of the spectroscopic working bandwidth $\Delta\omega'$ to the characteristic spectral resolution [14]. In essence, the working finesse gives the maximum number of spectral lines resolvable by a spectroscopic setup using such slow-light waveguides.

$$\mathscr{F}_W \equiv \left\langle \frac{n_g}{c\alpha} \right\rangle \Delta\omega'. \tag{1}$$

Here, the working bandwidth is defined as the frequency range over which the spectral resolution does not change by more than 10% of its average value. This is, in general, different from the bandwidth discussed in the previous section because the loss is also frequency-dependent.

Photonic crystal waveguides are intrinsically lossless; loss in such systems is induced by disorder [23]. Inevitably, the fabrication process will be imperfect, resulting in sidewall roughness and lithographic inaccuracies. Fields that sample this disorder will be scattered out of the desired mode. There are two components to this loss: out-of-plane radiation losses, which scale linearly with group index, and backscattering losses, which scale quadratically [24]. This scaling arises from an increased density of states (in 1 dimension, DOS $\equiv dk/d\omega$), which, in the case of backscattering, applies to both the forward and backward propagating modes. As such, this scaling is fundamental, and cannot be overcome. However, since scattering occurs only at the disorder sites, it is possible to engineer the distribution of the mode to minimize the field overlap with the hole boundaries, and hence minimize the loss.

Following [25], we express the loss as

$$\alpha = c_1 \gamma(k) n_g + c_2 \rho(k) n_g^2, \tag{2}$$

#184499 - $15.00 USD Received 4 Feb 2013; revised 6 Apr 2013; accepted 8 Apr 2013; published 16 Apr 2013

where $\gamma(k)$ and $\rho(k)$ are mode-dependent parameters involving integrals of the fields over the hole boundaries. Explicit formulas for $\gamma(k)$ and $\rho(k)$ are given in [25]. The constants c_1 and c_2 encapsulate technological parameters such as disorder and index contrasts and are to be used as fitting parameters to experimental data. For the purposes of this paper, we use the values of c_1 and c_2 determined by O'Faolain *et al.* [25], and calculate $\gamma(k)$ and $\rho(k)$ using a suitably-modified version of the code provided by Beggs and Schulz [26] for the freely-available software package MIT PHOTONIC BANDS (MPB) [27].

It should be noted here that this rather simplistic model does not take into account the effects of multiple scattering. If the backscattering coefficient is large, light will be backscattered multiple times as it propagates through the waveguide, leading to a break-down of the Beer-Lambert law [28] and the emergence of localization phenomena [29]. When the characteristic localization length is shorter than the waveguide, sharp resonances appear in the waveguide's transmission spectrum [30], which would be especially detrimental to the performance of a slow-light spectrometer. Therefore, the treatment presented here is strictly only valid for waveguides shorter than ~ 150 μm, and with moderate group-index values. This constraint is expected to relax as fabrication procedures improve.

4. Results and discussion

The structures we consider in this paper consist of a triangular lattice of air holes in an air-clad Si membrane of thickness 220 nm. The lattice constant is $a = 398$ nm, and the hole radius is $r = 0.286a$. For these parameters, the first band-gap of the bulk photonic crystal extends from 1321 to 1562 nm. To form the waveguide, one row of holes in the nearest-neighbor direction is removed. We have performed a rudimentary optimization of this geometry for both the group index bandwidth product and the working finesse by scanning over the radius r_1, and lateral shift s_1, of the holes adjacent to the line defect (Fig. 2). This optimization is by no means exhaustive, and can be extended to a larger parameter space (most commonly, the radii and shifts of the second and third row of holes).

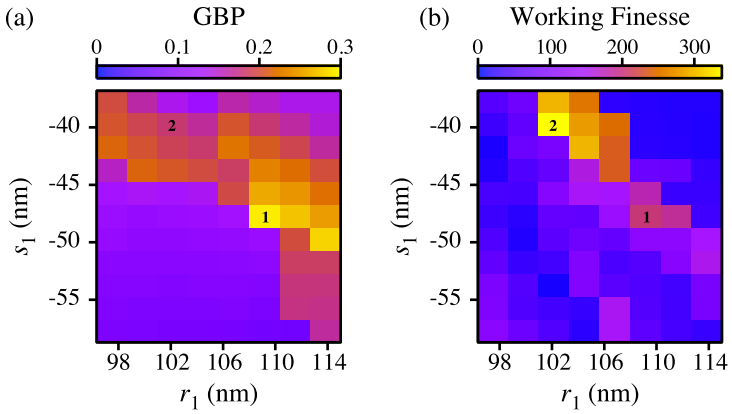

Fig. 2. Group index bandwidth product (a), and working finesse (b) of PhCWs for different values of the radius r_1, and lateral shift s_1, of the holes adjacent to the line defect. The designs corresponding to the maximum GBP and maximum $\mathscr{F}_W$ are labeled '1' and '2', respectively.

In Fig. 3, we compare the calculated group index, loss, and characteristic spectral resolution of two waveguides: the one with the maximum GBP ($r_1 = 109.5$ nm, $s_1 = -47.8$ nm) and that with the maximum $\mathscr{F}_W$ ($r_1 = 102$ nm, $s_1 = -39.8$ nm). Both waveguides present moderate

#184499 - $15.00 USD Received 4 Feb 2013; revised 6 Apr 2013; accepted 8 Apr 2013; published 16 Apr 2013

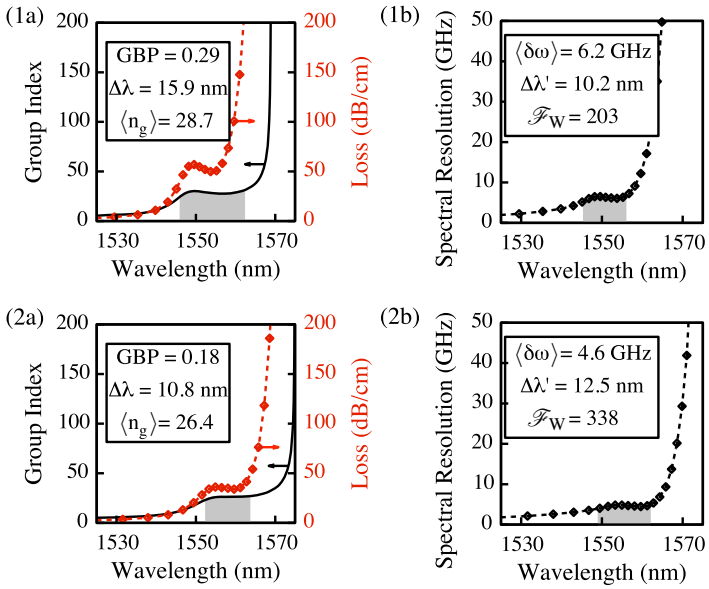

Fig. 3. Group-index profile and calculated propagation loss (a) and characteristic spectral resolution (b) of waveguides optimized for maximum GBP (1), and maximum working finesse $\mathscr{F}_W$ (2).

group-index values (28.7 and 26.4, respectively). Since the footprint of slow-light spectrometers scales as $1/n_g$, spectrometers based on these waveguides could have a footprint more than six times smaller than one based on conventional Si waveguides, whose group index is approximately 4, without suffering a degradation in spectral resolution. Comparing the two designs, however, one can see that for the first waveguide the associated propagation loss is higher over the entire working bandwidth. As a result, the second waveguide has both a finer characteristic spectral resolution (4.6 GHz, or 0.04 nm) and a wider spectral working bandwidth (12.5 nm), and can resolve 50% more spectral lines than the first one.

5. Conclusion

In this paper, we have investigated the applicability of photonic crystal waveguides to high-resolution on-chip spectrometers. We have proposed a new optimization metric, the working finesse, which relates to the maximum number of spectral lines a slow-light spectrometer can resolve. Through numerical simulation, we have shown that a photonic crystal waveguide optimized for working finesse could form the basis of a spectrometer with a spectral resolution of 0.04 nm over a 12.5 nm bandwidth while allowing for a sixfold reduction of the device's footprint. Even better performance could be achieved by further optimizing the waveguide geometry.

Acknowledgements

The authors would like to acknowledge many useful discussions with Joseph E. Vornehm and Sebastian A. Schulz. This work was supported by the US Defense Threat Reduction Agency-Joint Science and Technology Office for Chemical and Biological Defense (Grant No. HDTRA1-10- 1-0025) and by the Canada Excellence Research Chairs Program.

#184499 - $15.00 USD Received 4 Feb 2013; revised 6 Apr 2013; accepted 8 Apr 2013; published 16 Apr 2013